PHYSICAL REVIEW B VOLUME 16, NUMBER 8 15 OCTOBER 1977

Infrared and Raman spectra of the silicon-hydrogen bonds in amorphous silicon prepared by glow discharge and sputtering

M. H. Brodsky, Manuel Cardona,* and J. J. Cuomo
IBM Thomas J. Watson Research Center, Yorktown Heights, New York 10598
(Received 15 April 1977)

We have studied the number and nature of the silicon-hydrogen bonds in amorphous silicon films prepared in plasmas either of silane or of hydrogen and argon. The films from silane glow discharges have qualitatively different Raman and infrared spectra which depend on deposition parameters such as substrate temperature and silane gas pressure. Three main groups of spectral bands are seen associated with the Si-H bonds: the Si-H bond stretch bands, the bands due to relative bending of two or three Si-H bonds with a common silicon atom, and the "wagging" bands of Si-H bonds with respect to the Si matrix. These bands are split in a way suggestive of the presence of SiH, SiH_2, and SiH_3 complexes: the bond-bending bands are absent when only SiH bonds are present. All three types of complexes are identified in films deposited from glow discharges of silane at pressures ~ 1 Torr and room temperature. Higher substrate temperatures and/or lower pressures reduce the SiH_2 and SiH_3 concentrations: films deposited at 250°C and 0.1 Torr contain only SiH groups. From the strength of the corresponding absorption bands, H concentrations as high as 35 to 52 atomic percent are estimated. Films sputtered at 200°C in a 10% H_2-90% Ar mixture contain all three groupings observed in the silane-derived samples. Deuterated sputtered films are used to confirm the analysis. The first- and second-order Raman scattering spectra of the Si-Si bonds in pure and hydrogenated a-Si are also discussed. The scattering efficiency of a-Si is found to be as much as 10 times that of crystal Si. The depolarization ratio of the a-Si Raman spectrum has been remeasured. Finally, a picture is presented of when it is appropriate to refer to heavily hydrogenated a-Si as still being a material describable by a-Si network models.

I. INTRODUCTION

Pure amorphous Si (a-Si) or Ge (a-Ge) films as normally prepared by evaporation, sputtering, or ion bombardment, are quite different in terms of their optical and electrical properties from a-Si or a-Ge chemically deposited from Si- or Ge-bearing compounds, usually hydrides and, on occasion, halides.[1] Presumably the basic difference between the "normal" and " chemical" methods is that the "normal" depositions give films permeated with paramagnetic dangling bonds of the order of 10^{20} per cm^3, as seen by electron-spin-resonance (ESR)[2] and bulk-magnetic-susceptibility[3-5] measurements. These dangling bonds are most likely associated with small multivacancy complexes[6,7] (divacancies, trivacancies, etc.) within the disordered tetrahedrally coordinated network believed to be characteristic of either type of preparation as evidenced by similar diffraction patterns[8,9] and vibrational spectra.[10] The "chemical" methods, such as glow-discharge decomposition[6] or reactive sputtering in hydrogen,[11] give films with considerably lower concentrations of paramagnetic dangling bonds,[3-7,11,12] less than 10^{16} cm^{-3} in some cases.[13] The dangling bonds are presumably saturated by hydrogen atoms introduced into the film during preparation.

This presumption has not always been accepted for a-Si produced from glow discharges of silane (SiH_4). Early infrared (ir) studies did not show any bonded hydrogen[14] and later such evidence was found only in films prepared below 400 K.[12,15] However, we feel that the bulk of the evidence now is that hydrogen is indeed responsible for the passivation of dangling bonds and the concomitant changes in optical and electrical properties. For example, hydrogen can be added during sputtering depositions of a-Si or a-Ge to reproduce the key doping results[16,17] previously attained only with glow-discharge produced films.[18,19]

We report here measurements and identification of ir- and Raman-active vibrations in some silicon hydrides (silanes) and in hydrogenated and deuterated a-Si films. Results are given for a-Si films prepared (i) from glow discharges of silane, and (ii) by depositions from a silicon cathode sputtered with hydrogen-argon or deuterium-argon gas mixtures.

From the vibrational spectra we are able to identify a variety of hydrogen bonding sites corresponding to isolated SiH bonds as well as SiH_2 and SiH_3 groupings. Hereafter we use the notation Si-H to represent silicon-hydrogen bonds in any SiH_n grouping while SiH, SiH_2, and SiH_3 are reserved to the specific single, double, and triple groupings. Polarized and depolarized Raman spectra and the complementary ir spectra are compared with gas data for SiH_4, Si_2H_6, higher silanes, and halogen silanes in order to identify the stretching (~2000 cm^{-1}), bending (~900 cm^{-1}), and wagging (~600 cm^{-1}) modes. Substitution of deuterium for hydro-

gen confirms the identifications. In the glow-discharge process, lower substrate temperatures and higher silane pressures favor the SiH_2 and SiH_3 groupings and perhaps even polymerization[20]; we call such material amorphous silicon hydrides, a-SiH_x, or polysilanes, a-$(SiH_2)_n$. Higher substrate temperatures and/or lower pressures lead to hydrogen atoms bonded to separate silicon atoms within the a-Si network; we call this material amorphous hydrogenated silicon, a-Si:H. In practice, we have been able to prepare glow-discharge films with predominantly one or the other type of bonded hydrogen,[20] while in sputtering, mixtures of a-SiH_x and a-Si:H are generally obtained.

We attempt quantitative estimates of the total number of hydrogen-silicon bonds by comparing the integrated ir absorption strengths of the bond stretching absorption (~2000 cm^{-1}) with published data for SiH_4 gas and for higher silanes. The number of double and triple groups is similarly estimated from the bond bending structure (~900 cm^{-1}).

The ir spectra obtained are compared with data for hydrogenated single-crystal silicon surfaces[21] and for hydrogen- and deuterium-implanted crystalline silicon.[22,23] A comparison is also made with spectra obtained for anodically stained silicon produced electrochemically.[24]

The observed Raman spectra of hydrogenated a-Si have an intrinsic part very similar to that of pure a-Si except for a decrease in the relative strength of the longitudinal acoustic (LA) structure. These spectra, their depolarization ratios, and intensities are discussed. A similar discussion is given for the extrinsic features due to the Si-H bonds.

In Sec. II we describe the experimental procedures including the glow-discharge and sputtering parameters used. The sample characterization procedures are also given. The ir and Raman spectra are presented in Sec. III. In Sec. IV the spectra are discussed in terms of mode identification, quantitative analysis of the bonded hydrogen content, and correlation of the type of hydrogen sites with the film growth conditions. Section V contains the conclusions.

II. EXPERIMENTAL PROCEDURES

A variety of amorphous silicon films were prepared in each of two different types of deposition systems. One of these systems was an inductively-coupled radio-frequency (rf) glow-discharge apparatus for the plasma decomposition or polymerization of silane, SiH_4. The other was a biased rf diode system for reactive sputtering depositions in argon-hydrogen or argon-deuterium mixtures from a silicon cathode.

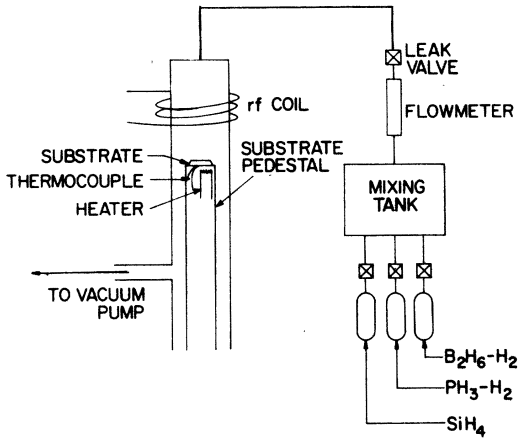

FIG. 1. Schematic diagram of glow-discharge apparatus for preparation of a-Si films from silane.

The glow-discharge apparatus, shown schematically in Fig. 1, is based on the systems described by Chittick[14] and by Spear and LeComber.[19] Silane is passed down a vertical 5-cm-diam quartz tube and flows by a 3-cm-diam temperature-controlled pedestal onto which a horizontal substrate is clamped so as to receive the deposited film. A glow-discharge plasma is excited in the flowing silane by a three-turn, 5-cm-long by 8-cm-diam, water-cooled coil driven by a 13.56-MHz radio transmitter. The power to the coil was estimated to be about 1 W. Smooth film deposition occurs when the gas pressure lies between about 10^{-2} and 1 Torr, as read by a Pirani gauge about 10 cm below the substrate pedestal. We estimate the absolute pressures of SiH_4 to be about half the nominal (air) readings of the Pirani gauge by occasional checks against a capacitance manometer. A rotary pump at the exhaust end of the apparatus provides for gas flow. The pressure is controlled by a leak valve at the gas intake. After passing through the plasma tube, the gas passes through an oven at 950 °C to decompose any residual SiH_4. Typical flow rates for 10^{-1} and 1 Torr are 0.2 and 5 cm^3/min(STP). If the rate is increased further we first get rough films and then for faster flows a yellowish powder "snows" out of the plasma. For this study, pedestal temperatures of either 25 or 250 °C were used.

The rf bias sputtering apparatus is shown schematically in Fig. 2. Its design was previously described.[25] Provision has been added for the introduction of hydrogen as well as the common dopant gasses (e.g., PH_3, B_2H_6) now in use in glow-discharge depositions. The cathode target is nominally intrinsic (99.999% purity) cast polycrystalline silicon which is bonded to a water-cooled copper plate. The sputtering region is determined by a 10.5-cm-diam ground shield. The substrates and

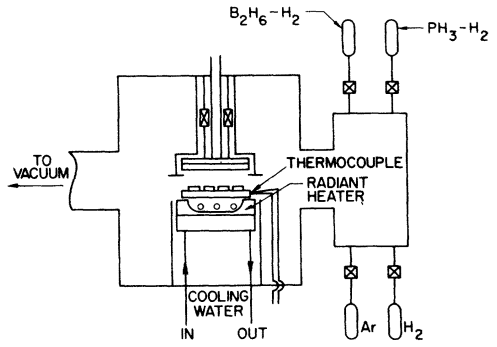

FIG. 2. Schematic diagram of rf bias sputtering apparatus for preparation of hydrogenated and deuterated a-Si films. For deuteration the H_2 cylinder is replaced by one containing D_2.

masks are mounted in a molybdenum holder within view of a radiant heater which is controlled by a thermocouple mounted inside the substrate holder. All deposits were made onto 200 °C substrates. Before sputtering, the chamber is evacuated to less than 6×10^{-8} Torr. The sputtering mixture is obtained by first adjusting the H_2 flow to the desired indicated partial pressure with an air-calibrated ion gauge; then the Ar flow is adjusted to give a total indicated pressure of 2×10^{-2} Torr. A pressure differential is maintained between the sputtering chamber and the diffusion pump by a nonsealing valve. In order to minimize oxygen contamination, the sputtering gases pass by a Ti-coated shroud at liquid-nitrogen temperature. In addition, experience has shown that a 50-Vrf bias applied to the substrate assists in further reducing the possibility of oxygen contamination. Table I summarizes the sputtering parameters.

The a-Si films were deposited through metal masks onto a variety of substrates. For the results reported here we used 2.5-cm-diam single-crystal silicon wafers with at least one optically polished face. The high-quality surfaces of commercially available Si wafers make them ideal substrates for Raman studies in a backscattering geometry. For ir transmission measurements, we generally used p-type, high-resistivity (>100 Ω cm) Si wafers polished on both sides and wedged in thickness so as to eliminate any interference fringe background from the substrate. Further, the index of refraction of crystal Si matches better the index of refraction of a-Si than most other ir transmitting materials; thus, the interference fringes from multiple reflections within the film are also minimized. Typical film areas were 1 × 2 cm.

TABLE I. Parameters used for the sputter depositions.

Target voltage	1700 V
Total pressure	2×10^{-2} Torr
Substrate temperature	200 °C
Applied substrate holder bias	50 V
Presputter time	30 min
Deposition time	60 min
Accumulation rate	2.7 Å/sec

All spectra reported here were gathered at room temperature. Most of the transmission data was measured in the ir region from 1 to 15 μm (10 000 to 667 cm^{-1}) with a Perkin-Elmer Model 21 Double Beam Spectrophotometer. For some samples spectra out to 50 μm (200 cm^{-1}) were taken with Perkin-Elmer Models 580 and 180 or Beckman Model 4260 Double Beam Spectrophotometers. All the transmission measurements were made relative to an uncoated reference Si substrate. The Raman spectrometer was a Spex Model 1401 double monochromator with holographic gratings. The measurements were performed with 250 mW of 5145 Å argon ion laser radiation in the backscattering configuration. The incident light was polarized in either the vertical or the horizontal plane, while the analyzer was kept fixed for horizontal polarization. The first-order Raman peak of crystalline Si was measured on an uncoated portion of the substrate in order to generate relative strengths of all scattered intensities.

The samples used for vibrational measurements were usually analyzed separately for purity and hydrogen content. In some cases, other samples either simultaneously or equivalently prepared were used for the parallel analysis. The details of the other methods of hydrogen analyses will be reported elsewhere.[26] The methods used included electron microprobe, mass spectroscopy of thermally evolved gases, and nuclear reactions involving protons. Comparisons between boron and phosphorus doped sputtered versus glow discharge films will also be discussed in a separate report.

III. RESULTS

A. Infrared spectra

We first present data for samples prepared by reactive sputtering in gas mixtures of nominally 10% H_2 (or D_2) and 90% Ar. Figure 3 shows the relative transmittances of approximately 1 μm thick films in the regions of Si-H or Si-D bond stretching, bending, and wagging frequencies. The transmittances in Fig. 3 are normalized to the absorption-free background transmittances in order to eliminate the shallow interference fringes due to the small index of refraction difference between the substrate ($n_{sub}\cong3.4$) and the films ($n_{film}\cong3.0$). To convert the transmittances to absorption coeffi-

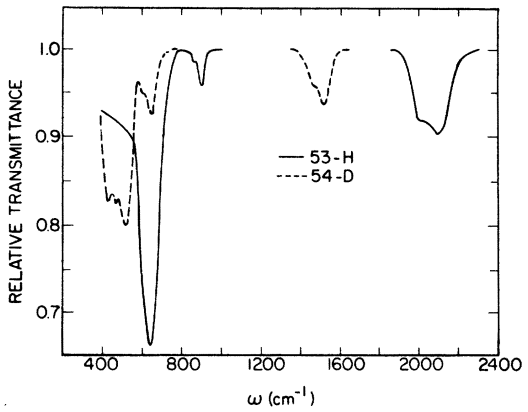

FIG. 3. Representative transmittance T versus frequency ω of ir spectra for two sputtered a-Si films. Sample No. 53-H was sputtered deposited by a mixture of 10% H_2 and 90% Ar, No. 54-D by a mixture of 10% D_2 and 90% Ar. The transmittances are shown relative to the absorption-free background transmittances of the same films.

cients, we approximate the interference free transmittance by

$$T=(1-R)^2e^{-\alpha d}/(1-R^2e^{-2\alpha d}), \tag{1}$$

where α is the absorption coefficient, d the film thickness, and R an empirically determined interface multiple reflection loss. We determine R by setting $T=T_0=0.54$ when $\alpha=0$. $T_0=0.54$ is the theoretical as well as experimentally checked transmission of the silicon substrates used. Equation (1) then becomes

$$T=\frac{4T_0^2e^{-\alpha d}}{(1+T_0)^2-(1-T_0)^2e^{-2\alpha d}}, \tag{2}$$

which can be solved for α in terms of the measured T. Although Eq. (1) is strictly true only for a freely supported film, and $T_0=0.54$ is true only when $n_{sub}=n_{film}=3.42$, we have verified for our case that Eq. (2) works well (±10% or better accuracy for α when $\alpha d>0.1$). Figures 4–7 show absorption coefficients versus wavenumber for different spectral regions of the transmission data of Fig. 3 for hydrogen-argon and deuterium-argon sputtered a-Si. Figure 4 shows the entire spectral range measured, while Figs. 5–7 are for the bond stretching, bond bending, and bond wagging regions, respectively. The basis for the identification of these three regimes will be discussed in Sec. IV below. For both hydrogen-argon and deuterium-argon sputtered a-Si, each of the three spectral regions has a doublet absorption consisting of two bands. In each doublet, the lower-frequency band is weaker and appears as a shoulder next to the higher-frequency peak.

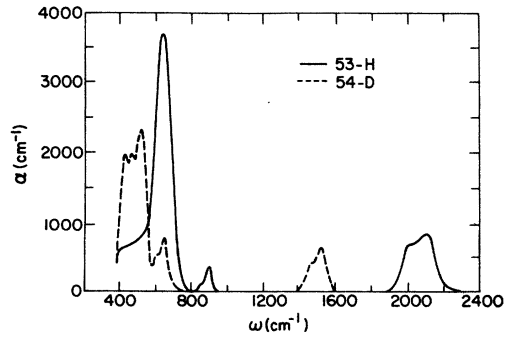

FIG. 4. ir absorption coefficient α versus wavenumber ω spectra for the same two sputtered a-Si films shown in Fig. 3.

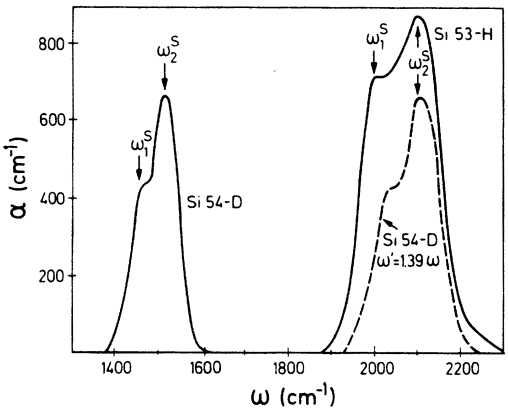

FIG. 5. Absorption coefficient α versus frequency ω for the Si-H and Si-D bond stretching bands for samples 53-H and 54-D (solid lines). The dashed line is the same 54-D spectrum with a new frequency axis ω' rescaled by a factor of 1.39.

Figure 5 shows the spectral regions appropriate to the stretching frequencies of Si-H and Si-D bonds. The solid curves in the 1900–2200 cm^{-1} and 1400–1600 cm^{-1} ranges are for the hydrogenated and

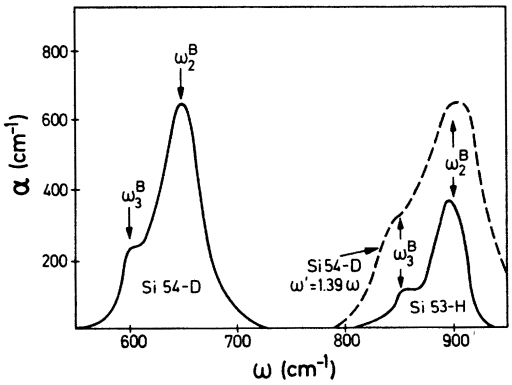

FIG. 6. Absorption coefficient α versus frequency ω for the Si-H and Si-D bond bending bands for samples 53-H and 54-D (solid lines). The dashed line is the same 54-D spectrum with a new frequency axis ω' rescaled by a factor of 1.39.

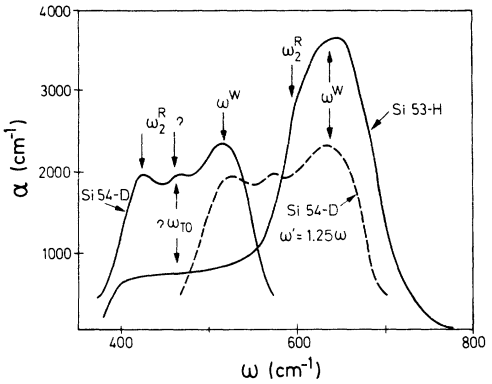

FIG. 7. Absorption coefficient α versus frequency ω for the Si-H and Si-D bond wagging (and rocking?) for samples 53-*H* and 54-*D* (solid lines). The dashed line is the same 54-*D* spectrum with a new frequency axis ω' rescaled by a factor of 1.25.

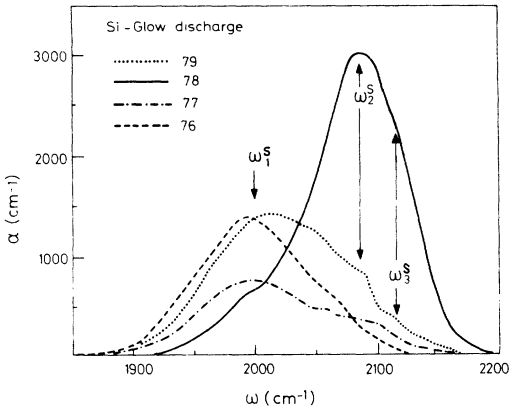

FIG. 8. Absorption coefficient α versus frequency ω for the Si-H bond-stretching bands for the four glow-discharge samples described in the text (see Table II).

deuterated samples, respectively. The dotted curve is the spectrum for the deuterated sample with a rescaled frequency axis. The frequencies have been rescaled by

$$\frac{\omega^S_{\text{Si-H}}}{\omega^S_{\text{Si-D}}} = \frac{2095\ \text{cm}^{-1}}{1510\ \text{cm}^{-1}} = 1.39, \tag{3}$$

so as to align the two higher-frequency peaks. Note that the scale factor 1.39 is about the square root of the ratio of the masses of D to H.

Figure 6 shows the spectral regions appropriate to the bending frequencies of Si-H and Si-D bonds. The solid curves in the 800–950 cm^{-1} and 600–700 cm^{-1} ranges are for the hydrogenated and deuterated samples, respectively. The dotted curve is the rescaled spectrum for the deuterated sample. Again, the frequency scale has been multiplied by 1.39 so that the $\omega^B_{\text{Si-D}} = 650\ \text{cm}^{-1}$ and the $\omega^B_{\text{Si-H}} = 895\ \text{cm}^{-1}$ peaks approximately line up.

Figure 7 shows the spectral regions appropriate to the wagging frequencies of Si-H and Si-D bonds. The solid curves in the 450–750 cm^{-1} and the 400–550 cm^{-1} ranges are for the hydrogenated and deuterated samples, respectively. The dotted curve is the shifted spectrum for the deuterated sample. This time the frequency scale has been multiplied by 1.25 so as to align the $\omega^W_{\text{Si-H}} = 640\ \text{cm}^{-1}$ and the $\omega^W_{\text{Si-D}} = 510\ \text{cm}^{-1}$ peaks.

Figures 8 and 9 contain the absorption coefficients versus wavenumber for four films of *a*-Si deposited from silane glow discharges. These films were deposited under four different combinations of substrate temperature and silane pressure, namely, Sample No. 78, low temperature (i.e., room temperature) and high pressure (i.e., 1.0 Torr); Sample No. 76, high temperature (250 °C) and low pressure (0.1 Torr); and the two intermediate cases of Sample No. 79, low temperature, low pressure; and Sample No. 77, high temperature, high pressure. The growth conditions and sample designations are summarized in Table II.

Figure 8 shows the 1900–2200 cm^{-1} spectral region appropriate to the bond stretching modes of SiH_n. Sample No. 78, grown at 1 Torr on a room-temperature substrate shows a strong peak at 2090 cm^{-1}, while the two samples deposited onto 250 °C substrates have absorption bands peaked

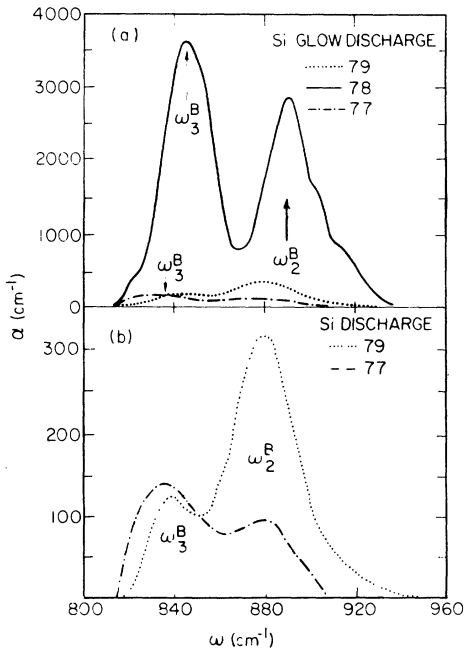

FIG. 9. (a) Absorption coefficient α versus frequency ω for the Si-H bond-bending bands for the same glow-discharge samples of Fig. 8. Sample No. 76 had no discernible absorption bands in this spectral region. (b) Enlarged presentation of the bond-bending bands for samples No. 77 and 79.

TABLE II. Summary of ir absorption data. The first four columns list the sample numbers, growth methods, gas pressures and substrate temperatures. The next three columns list the observed principal stretching, bending, and wagging frequencies. The strongest peaks of each band are underlined. The last two columns list the number of Si-H bonds found by integrating the stretching and bending absorption bands (see text). The asterisks indicate results for similar, but not identical, samples to those listed in the first column. The question marks indicate an inability to extract quantitative data because of a substrate absorption band.

	Growth parameters			Peak frequencies				
Sample number	Method	Gas pressure (Torr)	Substrate temp. (°C)	Stretch bands (cm^{-1})	Bend bands (cm^{-1})	Wag bands (cm^{-1})	No. Si-H bonds Stretch ($10^{22}/cm^3$)	Bend ($10^{22}/cm^3$)
53*H*	Sputtering	0.02	200	2095	895	640	2.1	0.4
or 33*H*	in H_2-Ar			2000	855	590		
54*D*	Sputtering	0.02	200	1510	650	515	2.3	?
or 38*D*	in D_2-Ar			1460	620	420		
78	Glow Disch.	1.0	25	2120	890	630*	3.3	3.2
	in SiH_4			2085	845	590*		
79	Glow Disch.	0.1	25	2000	880	635*	2.7	0.5
	in SiH_4			2020	840	590*		
76	Glow Disch.	0.1	250	2000	• • •	640*	2.3	~0.0
	in SiH_4					600*		
77	Glow Disch.	1.0	250	2085	880	640	1.5	0.1
	in SiH_4			2000	835	600*		

near 2000 cm^{-1}. The absorption band for the room-temperature, 0.1-Torr sample (No. 79), while weighted towards 2000 cm^{-1}, has some contribution from the 2090-cm^{-1} peak as well.

Figure 9 shows the 800–950 cm^{-1} spectral region appropriate to the bond bending modes of SiH_n. The room-temperature, 1-Torr sample (No. 78) has two well-separated absorption bands in this region at least an order of magnitude stronger than any of the other samples. The other extreme preparation condition, 250-°C substrate and 0.1-Torr silane, gave a sample (No. 76) with no detectable absorption in this spectral range, that is $\alpha_{peak} < 50$ cm^{-1}. As shown in Fig. 9(a), the two intermediate cases, samples Nos. 77 and 79, also have two bond bending absorption bands about an order of magnitude weaker than for the high-pressure, low-temperature sample. Figure 9(b) shows these smaller bands magnified so as to illustrate the switching of their relative strengths as well as the slight shifts in their frequencies.

Unfortunately, quantitative data were not obtained for the wagging-mode spectral range of these glow-discharge samples. However, we did observe qualitatively the wagging-mode absorption band at ~600 cm^{-1} in all these samples, as well as others similarly prepared. For example, Fig. 10 shows the relative transmittances for another set of glow-discharge samples which were grown at all four combinations of two temperatures (25 and 250 °C) and two pressures (0.09 and 0.5 Torr). In all samples, wagging modes are seen with slight shifts in the frequencies to higher values as the substrate temperature is increased or the silane pressure is decreased.

Table II summarizes the observed ir frequencies for the two sputtering and four different glow-discharge conditions. We note that some of these absorption bands due to Si-H and Si-D vibrations have

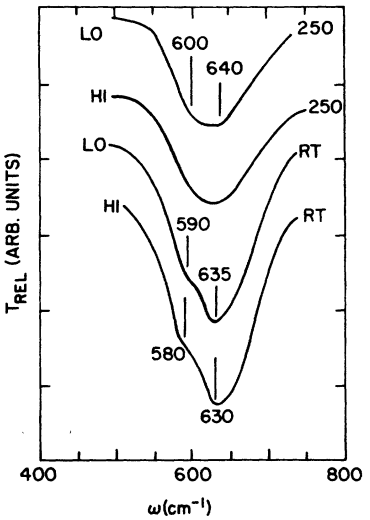

FIG. 10. Transmittance T versus frequency ω for the Si-H bond-wagging and rocking bands for four glow-discharge samples prepared under similar conditions to those of Figs. 8 and 9. LO and HI indicated low and high silane pressures during deposition onto either room-temperature (RT) or 250°-C substrates, as indicated. Three of the spectra are displaced for clarity of presentation.

been reported for crystal Si that has been ion implanted with H^+ and D^+,[22,23] exposed to nascent H,[21] or anodically stained in hydrofluoric acid.[24]

B. Raman spectra

The Raman spectra of four samples, "pure" *a*-Si prepared by sputtering in argon, a sample prepared by glow discharge under high pressure onto a substrate at room temperature (78), and two samples sputtered in argon with 10% of H_2 (33-*H*) or with 10% of D_2 (38-*D*), respectively, are shown in Fig. 11. The measurements were performed in the range of 200 to 2400 cm^{-1}. Additional measurements, to ascertain the possible presence of H_2 and D_2 in molecular form, perhaps inside voids, were performed in the range of the appropriate stretching vibrations (4156 cm^{-1} for H_2 and 2939 cm^{-1} for D_2).[27] In these ranges no signal was detected, an upper limit to the possible strength of the unobserved signal being 2 counts/sec, the strengths of the *a*-Si peak signal being typically 60 counts/sec. The linewidth expected for the H_2 stretching vibrations is 3.5 cm^{-1}.[28]

The data shown in Fig. 11 were obtained at room temperature in a backscattering configuration with parallel analyzer and polarizer. Almost all the samples exhibit the $\omega_{LA} = 300$ cm^{-1} longitudinal acoustical and the $\omega_{TO} = 480$ cm^{-1} transverse optical structure of *a*-Si.[10,29] The exception is Sample 78 for which no ω_{LA} structure is observed. The notation is that of the corresponding crystal modes. The ω_{LO} (longitudinal optical) shoulder was seen, as usual, faintly, in some of the samples around 380 cm^{-1}. The transverse acoustical ω_{TA} = 190 cm^{-1} structure was also seen but not studied in detail because of its being superimposed on a large Rayleigh background. The frequencies of the structures observed in Fig. 11 plus those of a glow-discharge sample (No. 92), prepared at 250 °C, and with an infrared spectrum very similar to that of Sample 79, are listed in Table III

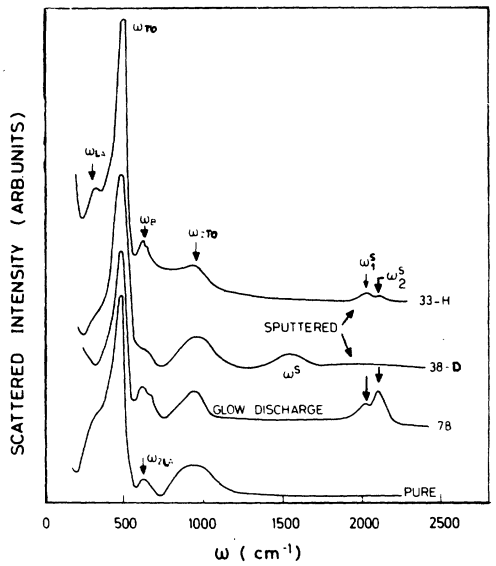

FIG. 11. Raman-scattered intensities versus frequency ω for four representative *a*-Si samples. The PURE sample was sputtered deposited in 100% Ar; the 33-*H* (38-*D*) samples were sputtered deposited in 90% Ar–10% H_2 (10% D_2). Sample 78 was deposited onto a room-temperature substrate from a high-pressure glow discharge of SiH_4.

TABLE III. Energies, intensities, and depolarization ratios ρ of the structure observed in the Raman spectrum of pure, hydrogenated, and deuterated *a*-Si. The intensities are integrated and divided by the *a*-Si intensity integrated between 200 and 600 cm^{-1}. $\omega_{LA} \simeq 300$ cm^{-1} has been omitted from the table. The frequency of the stronger peak of each ω^S doublet is underlined.

Sample	ω_{TO} (cm^{-1})	ρ	ω_{2LA}, ω^W (cm^{-1})	intensity	ρ	cm^{-1}	ω_{2TO} intensity	ρ	cm^{-1}	ω^S intensity	ρ
32 Pure (sputtered)	480	0.55	620	0.03	0.5	960	0.25	0.45	•••		•••
33-*H* (sputtered)	480	0.65	610 660	0.075	0.45	970	0.15	0.45	<u>2040</u> 2100	0.08	<0.3
38-*D* (sputtered)	480	0.52	610	0.03	0.5	960	0.3	•••	1500	0.12	0.2
92 Glow Disch. 250 °C Low press.	480	0.50	620 660	0.08	0.5	960	0.3	0.45	<u>2030</u> 2095	0.18	0.15
78 Glow Disch. 25 °C High press.	480	0.55	620 660	0.08	0.45	960	0.4	0.45	<u>2020</u> 2100	0.20	0.15

together with their strengths and depolarization ratios, to be discussed later. It is interesting to note that the ω_{TO} line peaks at 480 cm^{-1} in all samples measured. The ω_{LA} structure seems to become weaker relative to ω_{TO} along the sequence 32-(33*H* or 38*D*)-92-78, being nearly zero for Sample 78 (see Fig. 11). Along this sequence, the hydrogen content increases.

The line labeled ω_{2LA} occurs at 620 cm^{-1} in the pure and the deuterated samples for which it is weaker than the corresponding doublet observed in the hydrogenated samples (610–660 cm^{-1}). We thus conclude that the peak at 610 cm^{-1} is an overtone of the main *a*-Si ω_{LA} structure. The line observed at 660 cm^{-1}, a consequence of the presence of hydrogen, seems due to wagging (ω^W) vibrations of Si-H bonds, in correspondence with the structure observed in the infrared spectra. The structure labeled ω_{2TO} (960 cm^{-1}) is undoubtedly the overtone of the main *a*-Si ω_{TO} and seems to overwhelm any structure due to ω^B vibrations which should occur at the same frequency, although for Sample 78, that with the highest H_2 content, the ω_{2TO} structure is relatively stronger and may contain some contribution from ω^B vibrations. The only other structure observed can be related to the Si-H stretching vibrations (ω^S). It is a doublet with peaks at 2040 and 2100 cm^{-1} for sample 33*H* and at 2020 and 2100 cm^{-1} for Sample 78. The relative intensities of the two lines are reversed in samples 33*H* and 78. The deuterated sample (38*D*) has a broad line at 1500 cm^{-1} which, according to the reduced mass ratio of Si-H to Si-D should correspond to the lines given above; the doublet, however, is not resolved.

It is worth pointing out that ω^S structure has also been observed[22] in the Raman spectrum of H^+ and D^+ implanted silicon at 1460 and 1488 cm^{-1} (D^+) and at 2056 cm^{-1} (H^+), in reasonable agreement with our observations.

We have listed in Table III the frequencies of the observed Raman peaks, their depolarization ratios ρ (ratio of scattering efficiencies for parallel-perpendicular to parallel-parallel polarizer-analyzer configurations), and their strengths with respect to that of the main *a*-Si structures. The ω^S Si-H stretching vibrations are nearly completely polarized, as one would expect by comparison with the corresponding lines of disilane ($\rho \simeq 0.11$).[30] The average depolarization ratio found for the main *a*-Si peak is 0.55. This value is somewhat lower than that reported earlier (0.8).[10]

By comparison of the *a*-Si spectrum with the scattering from the [111] oriented, polished and etched crystalline substrate, we have determined the ratio of the *a*-Si integrated scattering between 200 and 600 cm^{-1} to that of the Raman-active phonon in the crystal. For pure (nonhydrogenated) sputtered *a*-Si the directly measured scattered intensity was 3 times smaller than for the crystal. In order to obtain a meaningful scattering efficiency or cross section we divide the measured values by the absorption length, i.e., multiply by the absorption coefficient (more nearly exactly, the sum of absorption coefficients for the incident and scattered radiation). For crystal Si we use the absorption data of Dash and Newman,[31] and for *a*-Si we use our own measurements performed on films deposited on sapphire substrates. For the sputtered *a*-Si, the sapphire substrates were side-by-side with the crystal wafer during deposition. For the glow-discharge samples, a separate run was necessary for each sapphire substrate. At the laser wavelength, the ratio of the amorphous to crystalline absorption coefficients is about 30. The net result we obtained is a Raman scattering efficiency for *a*-Si that is 10 times that of crystal Si. This scattering efficiency decreases with H content and reaches a value of 5 times that of crystal Si for sample No. 78. No correction was made for the different relative importances of the Bose-Einstein factors in the crystalline and amorphous spectra.

IV. DISCUSSION AND ANALYSIS

A. Identification of the observed infrared structure

Three groups of structures are expected for the vibration spectra of Si-H bonds: stretching (ω^S), bending (ω^B), and wagging or rocking (ω^W, ω^R), corresponding to the three rows of modes shown in Fig. 12. The ω^B modes are due to the forces opposing changes in the angles between Si-H bonds within SiH_2 or SiH_3 groups. Contrary to the stretching and wagging vibrations, the bending modes should be absent for Si atoms bonded to a single H, i.e., isolated SiH groups. Thus a measurement of the ratio of the ir absorption strength of the ω^B to the ω^S modes should give an indication of how much of the H is bonded to Si as isolated H atoms. It is also known that the frequency of the ω^S vibrations decreases slightly in going from triple H groups (ω_3^S) to single hydrogens (ω_1^S).[32]

In order to identify the ω^S, ω^B, and ω^W modes in hydrogenated *a*-Si we start with a discussion of the infrared absorption data available for silane SiH_4,[32,33] disilane $(SiH_3)_2$,[30] trisilane SiH_3-SiH_2-SiH_3,[34] *n*-tetrasilane $(SiH_3$-$SiH_2)_2$,[35] and iso-tetrasilane $(SiH_3)_3$-SiH.[35] The frequency of relevant structure observed in these gaseous compounds and their identification in terms of Fig. 12 is given in Table IV. We have also listed in this table the strength of the absorption bands as represented by the integral

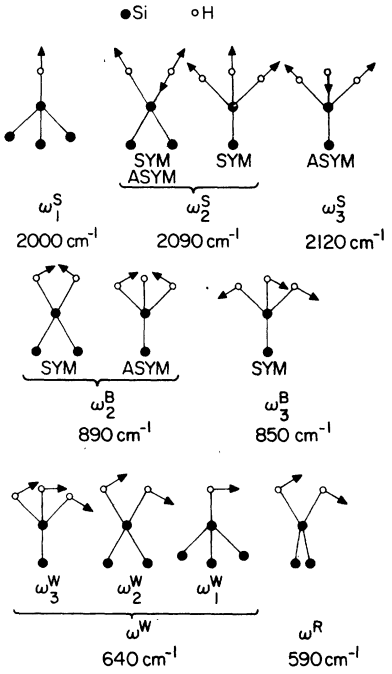

FIG. 12. Schematic illustration of the bond-streching (top row), bond-bending (middle row), and bond wagging and rocking (bottom row) modes of SiH, SiH_2 and SiH_3 groupings either in hydrogenated *a*-Si or gaseous silanes. The mode notation is described in the text. The frequencies in cm^{-1} are those seen in hydrogenated *a*-Si. SYM or ASYM indicate symmetric asymmetric modes. The solid circles represent Si atoms, the open circles represent H atoms. Only the relevant bonds to one central Si are shown, the other Si atoms can be connected to either Si or H atoms.

$$\Gamma = \frac{1}{NL}\int \ln\frac{I_0}{I}\frac{d\omega}{\omega} = \frac{1}{N}\int \frac{\alpha}{\omega}d\omega, \tag{4}$$

where L is the length of the gas cell, N the number of moles per unit volume, I_0 and I the incident and transmitted energy, respectively, and α the absorption coefficient. We express Γ in cm^2 per millimole (cm^2/mmol). The values of Γ have been determined accurately for SiH_4 by McKean.[36] Those for the higher order of silanes were obtained by integration of enlargements of the figures in Refs. 30, 34, and 35. They are, therefore, less accurate. It is clear from Table IV that one can take the strength of the ω^S lines as a measurement of the number of Si-H bonds, the corresponding dipole moment being almost independent of substance. We shall use this result, with the appropriate correction for the presence of the *a*-Si matrix, to determine the number of Si-H bonds in hydrogenated *a*-Si.

The stretching modes for the gaseous silanes listed in Table IV have three identifiable frequencies ω_1^S, ω_2^S, and ω_3^S. The lines ω_1^S and ω_3^S appear in all higher silanes as shoulders to the main ω_2^S line. Although it is not possible to estimate quantitatively the strengths of these lines, it appears that they are roughly proportional to the number of single (Si-H bonds) for ω_1^S and to that of triple Si-H bonds (SiH_3 groups) for ω_3^S. Note that ω_1^S appears only in $(SiH_3)_3$-SiH, for which compound ω_3^S is also relatively stronger than for $(SiH_3$-$SiH_2)_2$.[35] The identification of the three stretching frequencies ω_1^S, ω_2^S, ω_3^S with vibrations of single, double, and triple groupings of Si-H bonds follows

TABLE IV. ir frequencies in cm^{-1} and absorption strengths Γ in cm^2/m mole of the stretching, bending, and wagging modes and rocking modes in several silane gasses and the corresponding frequencies observed in glow discharge sample No. 78, sputtered hydrogenated samples No. 53-*H*, and sputtered deuterated sample No. 54-*D*. Where possible, the normalized strengths per bond (Γ^S/ζ) or per SiH_n group (Γ_2^B/ζ, Γ_3^B/ζ) are shown. For each molecule, ζ is the number of its SiH bonds or SiH_2 and/or SiH_3 groups contributing to the absorption process.

	ω_1^S	ω_2^S	ω_3^S	Γ^S	Γ^S/ζ	ω_2^B	Γ_2^B	Γ_2^B/ζ	ω_3^B	Γ_3^B	Γ_3^B/ζ	ω^W	Γ^ω	ω^R
SiH_4 [a]		2189		14	3.5	914			914	44				
$(SiH_3)_2$ [b]		2179	2190	22	3.7	940	19	10	844	60	30	625 [c]		
SiH_3-SiH_2-SiH_3 [d]		2180	2210	28	3.5	948	15	5	884	58	29	711	44	580
$(SiH_3$-$SiH_2)_2$ [e]		2155	2210	34	3.4	935	23	5	870	50	25	694	35	622
$(SiH_3)_3$-SiH [c]	2050	2155	2210	30	3.0	935	20	7	879	80	27	695	30	
a-Si 78	2000	2085	2120			890			845			630 [f]		
a-Si 53*H*	2000	2095				895			855			640		
a-Si 54*D*	1460	1510				650			515			510		420

[a] Reference 31(a).
[b] Reference 29.
[c] Raman mode.
[d] Reference 32.
[e] Reference 33.
[f] From Fig. 10, the RT, High-pressure sample.

from the arguments given above provided one also allows for a contribution of the triple bonds to ω_2^S as illustrated in Fig. 12 and discussed below. The ir active stretching vibration of the triple bond group should split into a symmetric and an asymmetric component[30,37]; the asymmetric component is expected to be higher than the symmetric one [see $(SiH_3)_2$ in Table IV]. Thus it is reasonable to attribute ω_3^S to the asymmetric component of the triple bond group stretch and ω_2^S to the symmetric one plus the double bond group stretch. While the double-bond group stretch should also split into symmetric and asymmetric components, we believe the splitting is too small to be seen. We note that for the corresponding C-H bonds in the alkanes, the symmetric-asymmetric splitting (70 cm^{-1}) of the double-bond group is smaller than for the triple-bond group (90 cm^{-1}).[37]

We divide the structure in the 2000-cm^{-1} region of the ir spectra of variously prepared *a*-Si films into three frequency bands analogous to the ω_1^S, ω_2^S, and ω_3^S bands of the Si-H stretching modes in the gaseous silanes. Because of solid-state effects, the frequencies in *a*-Si are 50–100 cm^{-1} lower than the corresponding frequencies in the gases (see Table IV). For example, for the room-temperature, high-pressure glow-discharge samples in Fig. 8, the SiH_3 asymmetric stretch ω_3^S lies at 2120 cm^{-1} and is seen as a shoulder on the dominant ω_2^S peak at 2085 cm^{-1}. We interpret the ω_2^S peak as having a sum of contributions from symmetric SiH_3 stretches as well as both symmetric and asymmetric SiH_2 stretches. Again in Fig. 8, the high-temperature, low-pressure sample has its dominant peak of $\omega_1^S = 2000$ cm^{-1} which we identify as a singly bonded SiH mode. The first row of Fig. 12 illustrates the different mode contributions to ω_1^S, ω_2^S, and ω_3^S along with the observed frequencies for hydrogenated *a*-Si.

The above illustrations for the glow-discharge samples show that we can, by control of the substrate temperature and silane pressure,[20] shift the hydrogen locations from multiply grouped SiH_3 and SiH_2 sites (ω_2^S and ω_3^S bands) to isolated SiH sites (the ω_1^S mode). For the sputtered films, however, we have not achieved such control. As shown in Fig. 5, both the strong ω_2^S and a strong ω_1^S bands are present in comparable strengths. Connell and Pawlik[11] also report a stretching doublet for all hydrogenated sputtered *a*-Si and *a*-Ge films; however, their interpretation of the origin of the two principal frequencies differs from ours. They postulate two possible H sites, namely, (i) on the surfaces of voids, and (ii) within the amorphous network, whereas our identification in terms of SiH_n groups is based on the known structure of the gaseous silanes and analogous hydrocarbons.

Hydrogen triply grouped with a SiH_3 should show two ir modes due to the changes in the relative angles between the bonds. One of these modes is the symmetric bending mode (see Fig. 12, ω_3^B) while the other is asymmetric (one of the two ω_2^B in Fig. 12, sometimes called a "deformation mode").[30] For doubly bonded hydrogen in SiH_2, however, there should only be one bending mode (the other ω_2^B in Fig. 12). We have made this grouping of the two ω_2^B modes because we expect the symmetric bending ("deformation") mode of triply grouped hydrogen to have a frequency close to that of the bending mode of double grouped hydrogen. It is thus possible to explain the two ω^B lines listed in Table IV in the following manner: ω_2^B encompasses the two-bond bending and the asymmetric three-bond bending. Hence ω_3^B is exclusively the symmetric three-bond bending. It follows that ω_3^B appears stronger in $(SiH_3)_3$-SiH than in $(SiH_3\text{-}SiH_2)_2$. It is therefore reasonable to associate the 890 cm^{-1} absorption band of hydrogenated *a*-Si to ω_2^B and that a 850 cm^{-1} to ω_3^B. Bond-bending structures should, of course, be absent when H is only singly grouped in *a*-Si. This has been shown to be the case for Sample 76, for which only the ω_1^S structure is present. The ratio strengths of ω_2^B to ω_3^B should allow us to estimate the relative proportion of double to triple H sites. Thus from Fig. 9, we immediately conclude that Sample 79 has a higher proportion of double bonds than either Samples 77 and 78, although the total number of double plus triple H groups is higher for Sample 78 than the others.

The situation in the 500–700 cm^{-1} region is not as clear as that presented above. On one hand the data in Refs. 30 and 35 do not go below 600 cm^{-1}. On the other hand, we were not able to measure all of our samples in this region before they were destroyed during other analysis measurements. We identify the line seen around 700 cm^{-1} in trisilane and the tetrasilanes (Table IV) with the wagging of the hydrogen in the triple complex SiH_3 with respect to the matrix (ω_3^W in Fig. 12). We also believe the single SiH bond should have a wagging frequency ω_1^W around 680 cm^{-1} in $(SiH_3)_3$-SiH and thus overlap with ω_3^W. The argument for the gases is as follows. Let us consider the compounds $HSiCl_3$ and $HSiBr_3$, with "wagging" frequencies 799 and 779 cm^{-1}, respectively.[38] Using the electronegativities of Cl(3.0), Br(2.8), and Si(1.8) we can estimate by extrapolation[39] the wagging frequency of the single H bond in Si_3-SiH to be 679 cm^{-1} which is close to the observed 695 cm^{-1}. The corresponding SiH_2 vibrations split into two modes referred to as wagging and rocking, ω_2^W and ω_2^R, as shown in Fig. 12. We believe by comparison with the halogenated silanes (e.g., Cl_2SiH_2)[40] that

the lines observed around 600 cm^{-1} for trisilane and n-tetrasilane are due to the SiH_2 rock. In glow-discharge samples similar to Nos. 76–79, we here have tentatively identified $\omega_3^W \approx \omega_2^W \approx 635$ cm^{-1}, $\omega_1^W \approx 625$ cm^{-1}, and $\omega_2^R = 590$ cm^{-1}. (See Fig. 10.). The rock mode seems to correspond to the line observed in a-Si-38D at 420 cm^{-1} after correction for the D to H mass ratio. In a-Si-33H this line is expected to overlap the weak ω_{TO} line seen at 480 cm^{-1} and thus may be difficult to resolve.

As we have already noted the Si-H ir spectrum observed in hydrogen-exposed crystal Si surfaces can be related to our interpretation of SiH, SiH_2, and SiH_3 features in the stretching bands. For example, Beckmann[24] prepared stain films on crystal Si by anodization in aqueous solutions of hydrofluoric acid. These films, which he identified as SiH_x, showed strong absorption peaks at 2090 and 2115 cm^{-1} and a weaker peak at 2135 cm^{-1}. Referring to Fig. 12, we identify these peaks with ω_1^S, ω_2^S, and ω_3^S, respectively. The slightly higher frequencies, particularly for ω_1^S, must have to do with the surface location of the Si-H bonds. Similar absorption frequencies have been observed by Becker and Gobeli[21] upon exposure of clean cleaved crystal Si surfaces to atomic hydrogen. They first saw an absorption band at 2060 cm^{-1} with H exposure, which grew in strength and shifted to 2105 cm^{-1} upon subsequent H-ion bombardment. Ion implantation of H^+ and D^+ into crystal Si also has been studied by ir spectroscopy, mostly in the region of the stretch bands.[22,23] While more complicated because of the variety of crystal-lattice environments, the Si-H and Si-D stretch bands observed for implanted crystals are analogous to those reported here for hydrogenated a-Si.

B. Integrated absorption versus concentration

The contribution of a given ir-active vibration of a Si-H band of frequency ω_t to the dielectric constant is[11]:

$$\Delta\epsilon(\omega) = \frac{4\pi N e_S^{*2}/\mu}{\omega_t^2 - \omega^2 - i\gamma\omega}, \tag{5}$$

where N is the number of such bonds per unit volume, γ the linewidth factor, μ the reduced mass, and e_S^* the appropriate effective charge for Si-H in solid a-Si. By integrating $\omega\Delta\epsilon$ over the absorption band of interest one obtains the well-known sum rule:

$$N = \frac{1}{2\pi^2}\frac{\mu}{e_S^{*2}}\int \omega \mathrm{Im}\Delta\epsilon\, d\omega = \frac{cn}{2\pi^2}\frac{\mu}{e_S^{*2}}\int \alpha(\omega)\, d\omega,$$

or

$$N = \frac{cn\omega_t}{2\pi^2}\frac{\mu}{e_S^{*2}}\int \frac{\alpha(\omega)}{\omega} d\omega, \tag{6}$$

where c is the speed of light, n the refractive index assumed to be frequency independent. Here α is the absorption coefficient due to $\Delta\epsilon$. Thus N, the number of bonds, can be determined from the integrated absorption provided e_S^* is known. By applying Eq. (6) to a dilute gas ($n \simeq 1$) we find

$$\frac{e_C^{*2}}{\mu} = \frac{c\omega_t}{2\pi^2 N_A}\frac{\Gamma}{\zeta}, \tag{7}$$

where Γ has been defined in Eq. (1), N_A is Avogadro's number, and ζ the number of relevant bonds per molecule. Equation (7) cannot be used directly to determine e_S^* because in the solid the local field differs from the applied field: a local-field correction must be made. Connell and Pawlik[11] used a Szigeti-type correction:

$$e_S^* = \tfrac{1}{3}(\epsilon_m + 2)e_C^*, \tag{8}$$

where ϵ_m is the electronic dielectric constant of the medium. The idea behind this correction is that the solid is a homogeneous medium composed of isotropically distributed polarizable dipoles, all with the same *ionic* and *electronic* polarizabilities. The local field is calculated by removing one dipole and drawing a sphere around it whose polarization charges determine the local-field correction. We believe this procedure to be inaccurate for hydrogenated a-Si which is not a homogeneous material of only Si-H bonds, but may rather be assumed to consist of Si-H bonds inbedded in an a-Si matrix. The Si-H bonds have nearly zero electronic polarizability, while that of the matrix is large. The expression for the effective dielectric constant of a medium composed of spheres in a matrix has been given by Genzel and Martin.[41] For the case of noninteracting spheres (a reasonable approximation in most of our samples) they find

$$e_S^{*2} = \frac{9\epsilon_m^2}{(\epsilon_0 + 2\epsilon_m)(\epsilon_\infty + 2\epsilon_m)} e_C^{*2}, \tag{9}$$

where ϵ_m is the dielectric constant of the matrix and ϵ_0 and ϵ_∞ are the static and ir dielectric constants of the Si-H bonds within the effective volume they occupy. Since Si-H bonds do not absorb in the visible, we set $\epsilon_\infty \approx 1$. A simple calculation using the data of Table IV and the atomic volume of Si shows that $\epsilon_0 \simeq \epsilon_\infty \approx 1$. Equation (9) thus becomes

$$\epsilon_S^{*2} \simeq \frac{9\epsilon_m^2}{(1 + 2\epsilon_m)^2} e_C^{*2}. \tag{10}$$

The enhancement factor of Eq. (10) represents the enhancement of the local field with respect to the macroscopic field for a *spherical* void inside of a medium of dielectric constant ϵ_m. It is possible to modify Eq. (10) so as to treat also ellipsoidal bonds.[41]

One may argue that while Eq. (10) can be used in

TABLE V. Szigeti and embedded sphere corrections to e_s^{*2} for media with relative electronic dielectric constants ϵ_m. See text, Eqs. (8) and (10).

ϵ_m	$\left(\frac{\epsilon_m+2}{3}\right)^2$	$\left(\frac{3\epsilon_m}{2\epsilon_m+1}\right)^2$
4	4.0	1.78
6	7.1	1.92
8	11.1	1.99
10	16.0	2.04
12	21.7	2.07
14	28.4	2.10
16	36.0	2.12

the limit of low H concentration, for high H concentration (Sample 78) the material is actually homogeneous polysilane and hence a Szigeti-type local-field correction [Eq. (8)] may not be too inaccurate. In this case $\epsilon_m = 6.5$ and the difference between the two corrections is a factor of 4 (see Table V). For the larger $\epsilon_m = 12$ appropriate to a-Si, the difference between both types of corrections reaches an order of magnitude and would be even larger for a-Ge where $\epsilon_m = 16$. Combining Eqs. (6), (7), and (10), we find:

$$N = \frac{(1+2\epsilon_m)^2}{9\epsilon_m^2} \frac{N_A n}{(\Gamma/\zeta)} \int \frac{\alpha(\omega)}{\omega}\, dw\,. \tag{11}$$

Table IV suggests that for the ω^S modes Γ/ζ is roughly the same for all silanes. Similar conclusions hold for doubly and triply bonded hydrogen in alkanes, but single C-H bonds seem to have a much smaller Γ_S.[37] The Γ of C-H bonds also depends strongly on the other neighboring C bonds. We are not able to ascertain to what extent this may also happen in the silanes, but we shall assume that all groupings of Si-H bonds, single, double, and triple, have the same value of $\Gamma/\zeta = 3.5$. We use for Γ the values determined for SiH_4, with $\zeta = 4$ where there are 4 Si-H bonds. We thus find the number N_S of Si-H bonds contributing to the stretching absorption band as

$$N_S = A \times 1.72 \times 10^{20}\ \text{cm}^{-2} \int_{\omega^S} \frac{\alpha(\omega)}{\omega}\, d\omega\,, \tag{12}$$

where

$$A = (1+2\epsilon_m)^2(\epsilon_m)^{1/2}/9\epsilon_m^2\,.$$

The values of N_S for our films appear in the next to last column of Table II.

For the ω_2^B band we use Table IV to obtain the average value of $\Gamma_2^B/\zeta = 7$ cm^2/mmol per SiH_2 or SiH_3 group present in the di-, tri-, or tetrasilane gases. We thus find for the number of $N_{d,t}$ of double and/or triple groups of hydrogen

$$N_{d,t} = A \times (8.6 \times 10^{19}\ \text{cm}^{-2}) \times \int_{\omega_2^B} \frac{\alpha(\omega)}{\omega}\, d\omega\,. \tag{13a}$$

For the ω_3^B band, Table IV shows that the average $\Gamma_3^B/\zeta = 28$ cm^2/mmol for the contribution of each SiH_3 in the same gases. It follows from Eq. (11) that the number N_t of triple groups of hydrogen is

$$N_t = A \times (2.1 \times 10^{19}\ \text{cm}^{-2}) \times \int_{\omega_3^B} \frac{\alpha(\omega)}{\omega}\, d\omega\,. \tag{13b}$$

While Eq. (13b) can be directly used to compute the total number of Si-H bonds in SiH_3 groups, i.e., $3N_t$, such a simplification for the result of Eq. (13a) is more difficult. This is because we have to estimate the relative contributions of the symmetric SiH_2 bend and the asymmetric SiH_3 bend (See Fig. 12) to Γ_2^B/ζ. By comparing the two tetrasilanes, we see that the SiH_2 groups contributes with about 70% of the strength of the SiH_3 contribution. Thus $N_{d,t} = N_t + 0.7N_d$, where N_d is the number of SiH_2 groups. The results of Eqs. (13) can now be used to find $N_d = (N_{d,t} - N_t)/0.7$. The total number of Si-H bonds contributing to the ω_2^B and ω_3^B bands is $3N_t + 2N_d$ and this result for each of our a-Si films appears in the last column of Table II.

It would be even more difficult to estimate the number of Si-H bonds associated with the ω^W wagging band. If, as postulated, the ω^W band has contributions from SiH_1, SiH_2, and SiH_3 groups, then on a per bond basis it is not clear that each SiH should contribute 2 and 3 times as much as each SiH_2 and SiH_3. Thus, from the Γ_1^W of Table IV we are unable to extract a unique value of Γ_1^W/ζ to use for hydrogenated a-Si.

The last two columns of Table II contain the results of performing the integrals in Eqs. (12) and (13) over the bond stretching and bending absorptions bands. It is seen that the number of Si-H stretching bonds of order 2 to 3×10^{22} bonds/cm^3 for either films sputtered in 10% H_2–90% Ar or deposited from SiH_4 glow discharges. Higher substrate temperatures lower the hydrogen concentration somewhat, but even glow-discharge films grown at 250 °C have about 1.5×10^{22} Si-H bonds/cm^3 implying about 24 at.% H for film densities[26,42] equal to 95% of the crystalline Si density of 5.0 $\times 10^{22}$ atoms/cm^3. We expect our quantitative results to be accurate to within a factor of 2. The biggest uncertainties are in the scaling of e_S^* to account for local-field corrections, which is more likely to give an overestimate of N_S. Thus the lowest-concentration sample (No. 76) has between 14 to 24 at.% hydrogen. For Sample 78, which has the highest estimated Si-H concentration of 3.3 $\times 10^{22}$ cm^{-3} and an estimated Si density[26,42] of 60% of the crystalline Si density, the estimated H concentration is 52 at.% from the strict application of Eq. (12). Again allowing for up to a factor of 2 overestimate in the local-field corrections, the

highest H concentration we measure is between 35 and 52 at.%.

As pointed out above, our scaling of e_S^* differs from that of Connell and Pawlik[11] who studied hydrogenated a-Ge, with some mention of a-Si. For the same absorption strengths, our formula [Eq. (12)] gives larger H concentrations than their Eq. (3) because we argue for a smaller local-field enhancement (see Table V). Further, we deduce our concentrations of total bonded H directly from the absorption bands of the stretching modes as all of the bonded H contributes to the absorption of the stretching band. Connell and Pawlik claim to use the bending modes for their concentration estimates. We have shown that the presence or absence of bending modes depends on how the H is grouped about the Si or, in their case, Ge, atoms. Also we point out that their identification of the absorption bands differs somewhat from ours in that their 0.07 eV (565 cm^{-1}) band is, in our identification scheme, due to wagging not bending modes.

We have had our films analyzed for the total H content by the nuclear resonance reaction of 6.385-MeV ^{15}N ions with protons.[43] The detailed results of the nuclear analysis are published separately,[26] but we quote here the fact that for any film analyzed the total H content determined by nuclear analysis is generally about 50 percent lower then the numbers shown in Table II for the bonded H content as determined from the integrated absorption strength of the stretch band. This supports our contention that Eq. (11) is a reasonable estimate of the number of Si-H bonds, albeit slightly on the high side because of the simplified form of Eq. (10). Further, the nuclear analysis, which counts all H atoms, bonded or not, in combination with the same order of magnitude result from ir absorption, indicates that essentially all the H is bonded to Si. This is in agreement with the null result in our attempt to see molecular H_2 by Raman scattering.

C. Deuterated compared with hydrogenated a-Si

A comparison of the ir spectra of sputtered deuterated and hydrogenated samples has been shown in Figs. 5–7 for the stretching, bending, and wagging vibrations, respectively. The features of the deuterated sample can be brought to coincide with the corresponding features of the hydrogenated one by multiplying the energy scale by a factor of 1.39 for Figs. 5 and 6, and 1.25 for the wagging bands of Fig. 7. The factor of 1.39 is reasonable since it agrees with the factor required to perform a similar transformation for the stretching and bending modes of disilane and equals the square root of the Si-H to Si-D reduced mass ratio. The reason why the ratio is smaller in Fig. 7 is probably the low frequency of the wagging modes: we note that ω^W for Si 54-D (510 cm^{-1}) falls only slightly above the ω_{TO} vibrations of the Si-Si matrix (480 cm^{-1}). Interaction between these two modes is expected to shift ω^W to higher frequencies and thus decrease the ratio $\omega^W(H)/\omega^W(D)$. A similar effect is observed[40] for SiH_2Cl_2 and SiD_2Cl_2 for the rocking modes. If we interpret the structure at 425 cm^{-1} in sample 54-D as ω_2^R, we obtain $\omega_2^R(H)/\omega_2^R(D) = \frac{590}{425} = 1.39$, in agreement with the factors of Figs. 5 and 6.

The ratio of the integrated strengths of a given set of modes for the same density of either hydrogen or deuterium can be estimated with Eq. (6). Under the reasonable assumption of an approximately isotopically independent e_S^*, one finds that the integrated intensity is inversely proportional to the reduced mass μ. Thus we would expect the bands of the hydrogenated sample in Figs. 5–7 to be twice as strong as those of the deuterated one since the samples were prepared under the same conditions. This is in agreement with the experiment.

D. Raman spectra

Before addressing the Si-H vibrations, we discuss first the features of the spectra of Fig. 11 which can be unambiguously attributed to Si-Si vibrations. The main peak near 480 cm^{-1}, has been ascribed to modes analogous to the high-density zone-edge TO vibrations of crystalline Si.[10,29,44] We note that this peak remains at the same position in all hydrogenated samples. In disilane gas $(SiH_3)_2$, the corresponding peak occurs at 434 cm^{-1} and in deuterated disilane $(SiD_3)_2$ it occurs at 408 cm^{-1}.[30] The shift to lower frequency in $(SiD_3)_2$ is probably due to interaction with the Si-D wagging modes as mentioned in Sec. IV C. Although we have not found any information on the corresponding Si-Si modes of higher-order silanes, our results lead us to expect a shift with increasing order from 434 cm^{-1} to higher frequencies. The ω_{LA} shoulder of Fig. 11 decreases in strength with increasing hydrogen content and seems to have disappeared in the "polysilane" sample No. 78. An interpretation of this result is possible in terms of Yndurian and Sen's[45] recent cluster–Bethe-lattice calculations of the density of vibrational states in a-Si. They show that the presence of closed rings of atoms is necessary for the existence of longitudinal modes (LA and LO). The corresponding transverse modes (TA and TO) are independent of the presence of rings. Thus the decrease of the LA shoulder with increasing hydrogenation and its disappearance in the "polysilane" can be related to the breaking of silicon rings in the amorphous Si Network. We also point out that our measurements and some more recent data[46] seem to indicate a decrease

in the 190 cm^{-1} peak (not shown in Fig. 11) with increasing H content. This feature, corresponding to the zone-edge TA modes of the crystal, is a consequence of the Si tetrahedral bonds and would be expected to be absent in a material composed only of polysilane strands.

Alben *et al*[44] have given an interpretation of the Raman spectrum of pure *a*-Si in terms of the induced bond polarizabilities α_i of model cylindrically symmetric bonds with three independent terms of the α_i tensors:

$$\vec{\vec{\alpha}}_1 = \sum_{l\Delta} [\vec{r}_\Delta(l)\vec{r}_\Delta(l) - \tfrac{1}{3}\vec{\vec{I}}]\vec{u}_l \circ \vec{r}_\Delta(l), \tag{14}$$

$$\vec{\vec{\alpha}}_2 = \sum_{l\Delta} \{\tfrac{1}{2}[\vec{r}_\Delta(l)\vec{u}_l + \vec{u}_l\vec{r}_\Delta(l)] - \tfrac{1}{3}\vec{\vec{I}}\}\vec{u}_l \circ \vec{r}_\Delta(l), \tag{15}$$

$$\vec{\vec{\alpha}}_3 = \sum_{l\Delta} \vec{\vec{I}}\vec{u}_l \circ \vec{r}_\Delta(l), \tag{16}$$

where $r_\Delta(l)$ is the Δth bond vector of the lth atom, I is the unit dyadic, and u_l is the displacement vector of the lth atom. The term α_3 is due exclusively to bond stretching representing the isotropic part of the polarizability tensor. It produces a Γ_1 scattering tensor and would thus yield polarized scattering in an amorphous material. It should not contribute to the first-order scattering (Γ_{25}) in crystalline Si. In Eqs. (14)–(16), α_1 is the only term which contributes to the first-order scattering of crystalline Si. It represents the asymmetric effect of bond stretching and thus yields a depolarized spectrum ($\rho = \frac{3}{4}$). The α_2 term is also depolarized, but contains, unfortunately, bond stretch and bond bend contributions and we believe it would be more instructive for the present case to decompose α_2 into a pure bond bend component by subtraction of the appropriate amount of α_1. Alben *et al*. intentionally chose the depolarized form for α_2 so that it does not contribute to the crystalline first-order scattering, a circumstance which is due to the cancellation of bond stretch and bond bend terms.

In Table III we show that the average depolarization ratio $\rho = 0.55$, which is to be compared with the previously reported[10] $\rho = 0.8 \pm 0.1$. Alben *et al*.[44] assumed a completely depolarized spectrum. They were thus able to ignore polarized contributions (α_3 in Eq. 16) to the induced polarizability. Our results show that a readjustment of the fit is necessary to include the additional polarized (Γ_1) contributions.

In order to interpret the large scattering efficiencies of *a*-Si, we invoke the α_2 and α_3 components of Eqs. (14)–(16), which do not contribute to the crystalline scattering. The TA-TO ratio observed experimentally and the depolarization ratio of 0.8 ± 0.1 assumed by Alben *et al*. led to $\alpha_3 = 0$ and then led them to give the α_2 mechanism one-third the strength of α_1. We do not know the shape of the polarized contribution, but it should be similar to the density of phonon states. By combining the α_1, α_2, and α_3 contributions it may be possible to explain the observed spectral shape, depolarization ratio, and strength of the amorphous spectrum with respect to crystal strength. This last point would simply require large α_2 and α_3 contributions which automatically would increase the calculated *a*-Si scattering strength withoug contributing to the crystalline spectrum.

An additional scattering contribution could also be found in the microscopic mechanisms which are responsible for α_1, the differential polarizability of crystal Si.[47,48] The microscopic mechanisms involve the E_1(3.48-eV) and E_2(4.3-eV) gaps, possibly with contributions of opposite signs. The separate E_1 and E_2 gaps lose their meaning in *a*-Si where only a simple broad optical absorption maximum around 3 to 4 eV is observed.[49,50] This could remove partial cancellation between the E_1 and E_2 contributions to the Raman tensor of crystalline Si and enhance the scattering cross section by a large factor.

In this respect it is also interesting to point out that the ratio of second-order to first-order Raman strengths is also higher in *a*-Si than in crystalline Si. From our measurements, those of Renucci *et al*.,[48] and those of Temple and Hathaway,[51] we find the relative second-order strengths of the 2TO and 2LA bands (normalized to the respective first-order TO strengths) are 0.25 and 0.03 for the pure *a*-Si of Fig. 11 compared with the smaller ratios of 0.1 and 0.007 for crystal Si (Table VI).

We now proceed with a discussion of the hydrogen-related Raman scattering. According to Bethe and Wilson,[30] the Si-H stretch Raman band of $(SiH_3)_2$ is 2.2 times stronger than that of the Si-Si stretch in the same compound. Thus a single Si-H bond scatters with a strength equal to $2.2/6 \simeq 0.4$ times that of a single Si-Si band. In amorphous *a*-Si with a Si density N_{Si} and a hydrogen concentration equal to αN_{Si}, we would expect, using the bond scattering ratio given above, the ratio of the Si-H to Si-Si

TABLE VI. Relative second-order Raman intensities for crystal and amorphous Si. In each case, the second-order intensity is normalized to the first-order intensity of the main TO peak in crystal Si.

	I(2TO)/I(TO)	I(2LA)/I(TO)
Pure *a*-Si[a]	0.25	0.03
Crystal Si[b]	0.1	0.007

[a] Figure 11.
[b] References 46 and 49.

scattering intensities to be

$$\frac{I(\omega^S)}{I(\mathrm{TO})} = \frac{\alpha N_{\mathrm{Si}}}{2N_{\mathrm{Si}} - \alpha\frac{1}{2}N_{\mathrm{Si}}} \times 0.4 = \frac{\alpha}{2 - \frac{1}{2}\alpha}\, 0.4 . \qquad (17)$$

For Si-78, with $\alpha \simeq 0.8$, Eq. (17) yields

$$I(\omega^S)/I(\mathrm{TO}) = 0.2 ,$$

in reasonable agreement with the results of Table III. From the data for $(SiH_3)_2$,[30] the ω^B band would be expected to have only an intensity 0.25 times that of the ω^S band even if *all* Si-H bands were of the SiH_2 and SiH_3 variety. Thus, the ω^B vibrations should be inobservable in Raman scattering because they occur at the same frequency as $\omega_{2\mathrm{TO}}$.

Again referring to the Raman spectrum of $(SiH_3)_2$, we find 0.04 for the relative strength (with respect to Si-Si) of the ω^W band for a *single* SiH bond. This is consistent with the observed increase in the relative strength of the $2\mathrm{LA} + \omega^W$ band from 0.03 in *a*-Si to 0.08 in the hydrogenated samples.

We should point out that the reversal in the relative strengths of the two ω^S features, ω_1^S and ω_2^S, or the Raman spectra (Fig. 11) from sample No. 33-*H* to No. 78 is similar to that observed in the infrared spectrum. However, for reasons not clear to us, the ω_1^S Raman peak occurs ≈ 20 cm^{-1} higher than the corresponding infrared line. A possible speculation is that of the local molecular symmetry of staggered Si-H bonds analogous to the D_{3d} symmetry of $(SiH_3)_2$ gives nondegenerate ir and Raman modes.[52]

V. CONCLUSIONS

Our study of the infrared absorption spectra of hydrogenated *a*-Si films has shown that the hydrogen can be incorporated either singly, doubly, or triply in SiH, SiH_2, or SiH_3 groups. Quantitative estimates of the absorption strength are consistent with essentially all the incorporated H bonded to Si atoms. The amount of bonded H in films prepared from silane glow discharges is typically as high as 35 to 52 at.% for room-temperature deposited films and 14 to 25 at.% in films deposited at 250 °C. The ratio of SiH_2 and SiH_3 to SiH sites can be minimized by increasing the substrate temperature and reducing the silane pressure for the glow-discharge method. For films sputtered by 10% H_2–90% Ar mixtures, comparable bonded hydrogen concentrations have been found, but all sites, SiH, SiH_2, and SiH_3, are seen even for 200-°C substrates. Identification of the various stretching, bending and wagging mode frequencies have been given along with confirming evidence obtained from deuterated *a*-Si. The Raman spectra show clear complementary Si-H vibrational bands in those spectral regions free of background contributions from the *a*-Si host. The *a*-Si host has first-order scattering efficiencies up to 10 times more than crystal Si. The second-order *a*-Si spectrum is further enhanced by about a factor of 3. An earlier estimate of the depolarization ratio ρ is reduced from 0.8 ± 0.1 to 0.55 ± 0.05.

The picture that emerges from this and related studies is that two types of glow-discharge prepared *a*-Si films can be produced. Either type is hydrogenated. In one case the H is primarily bonded at well dispersed, that is, different Si sites. For convenience we call this type of material true hydrogenated *a*-Si and use the nomenclature *a*-Si:H. Such *a*-Si:H is still recognizable as *a*-Si in that the vibrational spectra indicate the retention of the disordered but still interconnected Si network. This Si network persists despite the presence of at least 14 at.% H. The other case is that of H primarily incorporated within complexes of SiH_2 and SiH_3 groups as might be expected in a polymer of highly cross-linked $(SiH_2)_n$ strands. For convenience we refer to this material as a silicon hydride or "polysilane" and use the nomenclature *a*-SiH_x because it is no longer recognizable as *a*-Si. The cross-linking is not enough to give an identifiable interconnected Si network as generally envisioned in continuous random-network models. The sputtered films we have studied appear to be a mixture of *a*-Si:H and *a*-SiH_x.

Note added in proof. J. C. Knights, G. Lucovsky, and R. J. Nemanich have recently proposed a different interpretation of the two bond-bending modes at 850 and 890 cm^{-1}. They point out that one does not need any SiH_3 groups to account for the observation of two bonds, but rather adjacent pairs of SiH_2 groups will result in an appropriate splitting of the bond-bending frequencies. Otherwise they agree with our model of highly cross-linked $(SiH_2)_n$ strands for *a*-SiH_x.

ACKNOWLEDGMENTS

The authors thank M. Albert, J. Bradley, H. Breitschwerdt, P. Maurer, V. Mayne-Branton, and S. Ruffini for their technical assistance in the preparation and analysis of the films; D. Bermejo and J. E. Smith, Jr. for discussions of the Raman spectra; F. Cardone and J. Kuptsis for microprobe analyses; the Perkin-Elmer and Beckman Instruments Corporations for use of their instruments for some of the measurements; W. A. Lanford and J. F. Ziegler for permission to quote the nuclear analysis results.

*Permanent address: Max-Planck-Institut für Festkörperforschung, 7000 Stuttgart 80, Federal Republic of Germany.

[1]For examples of the early results from different preparations see M. H. Brodsky, J. Vac. Sci. Technol. 8, 125 (1971).

[2]M. H. Brodsky and R. S. Title, Phys. Rev. Lett. 23, 581 (1969).

[3]S. J. Hudgens, Phys. Rev. B 14, 1547 (1976).

[4]H. Fritzsche and S. J. Hudgens, *Proceedings of the Sixth International Conference on Amorphous and Liquid Semiconductors, Leningrad, 1975* (Nauka, Leningrad, 1976), p. 6.

[5]J. R. Pawlik, G. A. N. Connell, and D. Prober, in Ref. 4, p. 304.

[6]W. E. Spear, *Proceedings of the Fifth International Conference on Amorphous and Liquid Semiconductors, Garmisch-Partenkirchen, 1973* (Taylor and Francis, London, 1974), p. 1.

[7]M. H. Brodsky and R. S. Title, *Structure and Excitations of Amorphous Solids*, edited by G. Lucovsky and F. Galeener, AIP Conference Proceedings 31, 97 (1976).

[8]P. Chaudhari and J. F. Graczyk, in Ref. 6, p. 59.

[9]M. V. Coleman and D. J. D. Thomas, Phys. Status Solidi 24, K111 (1967).

[10]J. E. Smith, Jr., M. H. Brodsky, B. L. Crowder, M. I. Nathan, and A. Pinczuk, Phys. Rev. Lett. 26, 642 (1971).

[11]G. A. N. Connell and J. R. Pawlik, Phys. Rev. B 13, 787 (1976).

[12]P. G. LeComber, R. J. Loveland, W. E. Spear, and R. A. Vaughan, in Ref. 6, p. 245.

[13]R. S. Title and M. H. Brodsky, Proceedings of the Seventh International Conference on Amorphous and Liquid Semiconductors, Edinburgh, 1977 (unpublished).

[14]R. C. Chittick, J. Non-Cryst. Solids 3, 255 (1970).

[15]R. Fischer (private communication).

[16]W. Paul, A. J. Lewis, G. A. N. Connell, and T. D. Moustakas Solid State Commun. 20, 969 (1976).

[17]M. H. Brodsky and J. J. Cuomo. IBM Technical Disclosure Bulletin 19, 4802 (1977).

[18]W. E. Spear and P. G. LeComber, Solid State Commun. 17, 1193 (1975).

[19]W. E. Spear and P. G. LeComber, Philos. Mag. 33, 935 (1976).

[20]M. H. Brodsky, Thin Solid Films 40, L23 (1977).

[21]G. E. Becker and G. W. Gobeli, J. Chem. Phys. 38, 2942 (1963).

[22]D. M. Gruen, R. Varma, and R. B. Wright, J. Chem. Phys. 64, 5000 (1976).

[23]H. J. Stein, J. Electron. Mater. 4, 159 (1975).

[24]K. H. Beckmann, Surf. Sci. 3, 314 (1965).

[25]J. J. Cuomo and R. J. Gambino, J. Vac. Sci. Technol. 12, 79 (1975).

[26]M. H. Brodsky, M. A. Frisch, J. F. Ziegler, and W. A. Lanford, Appl. Phys. Lett. 30, 561 (1977).

[27]G. Herzberg, *The Infrared Spectra of Diatomic Molecules* (Van Nostrand, Princeton, 1950), Ch. II.

[28]T. Yoshino and H. J. Bernstein, J. Mol. Spectrosc. 2, 213 (1958).

[29]M. H. Brodsky, in *Light Scattering in Solids*, edited by M. Cardona (Springer-Verlag, Berlin, 1975), Ch. 5.

[30]G. W. Bethke and M. K. Wilson, J. Chem. Phys. 26, 1107 (1957).

[31]W. C. Dash and R. Newman, Phys. Rev. 99, 1151 (1955).

[32]L. J. Bellamy, *The Infrared Spectra of Complex Molecules* (Chapman and Hall, London, 1975), p. 380–1.

[33]R. S. Armstrong and R. J. H. Clark, J. Chem. Soc. Faraday II 72, 11 (1976).

[34]E. J. Spanier and A. G. MacDiarmid, Inorg. Chem. 1, 432 (1972).

[35]S. D. Gokhale and W. L. Jolly, Inorg. Chem. 3, 946 (1965).

[36]D. C. McKean, Chem. Commun. 147, (1966).

[37]Ref. 32, p. 14ff.

[38]M. L. Delwaulle and M. F. Francois, C. R. Acad. Sci. 230, 743 (1950).

[39]A. L. Smith and N. C. Angeletti, Spectrochim. Acta 15, 412 (1959).

[40]D. H. Christensen and O. F. Nelsen, J. Mol. Spectrosc. 27, 489 (1968).

[41]L. Genzel and T. P. Martin, Surf. Sci. 34, 33 (1973).

[42]J. C. Knights, AIP Conf. Proc. 31, 296 (1976).

[43]W. A. Lanford, H. P. Trautretter, J. F. Ziegler, and J. Keller, Appl. Phys. Lett. 28, 566 (1976).

[44]R. Alben, D. Weaire, J. E. Smith, Jr., and M. H. Brodsky, Phys. Rev. B 11, 2271 (1975).

[45]F. Yndurain and P. N. Sen, Phys. Rev. B 14, 531 (1976).

[46]D. Bermejo, M. H. Brodsky, and M. Cardona, Proceedings of the Seventh International Conference on Amorphous and Liquid Semiconductors, Edinburgh, 1977 (unpublished).

[47]S. Go, H. Bilz, and M. Cardona, Phys. Rev. Lett. 34, 580 (1975).

[48]J. B. Renucci, R. N. Tyte, and M. Cardona Phys. Rev. B 11, 3885 (1975).

[49]H. R. Philipp, J. Phys. Chem. Solids 32, 1935 (1971).

[50]D. T. Pierce and W. E. Spicer, Phys. Rev. B 5, 3017 (1972).

[51]P. A. Temple and C. E. Hathaway, Phys. Rev. B 7, 3685 (1973).

[52]G. Herzberg, *Infrared and Raman Spectra of Polyatomic Molecules* (Van Nostrand, Princeton, 1945), p. 114.